Trellis–Based Receivers for SC–FDMA Transmission over MIMO ISI Channels

Wolfgang H. Gerstacker[1], Patrick Nickel[1], Frank Obernosterer,
Uyen Ly Dang[1], Peter Gunreben[2], and Wolfgang Koch[1]
[1]Inst. for Mobile Communications, Univ. of Erlangen–Nuremberg, Germany, Email: {gersta,nickel,dang,koch}@LNT.de
[2]NXP Semiconductors, Nuremberg, Germany, Email: peter.gunreben@nxp.com

***Abstract*—For the uplink of the E–UTRA Long Term Evolution (LTE) system, single–carrier frequency–division multiple access (SC–FDMA) transmission has been selected. Frequency–domain linear and decision–feedback equalizers have been already given in the literature for an SC–FDMA transmission over a multiple–input multiple–output (MIMO) intersymbol interference (ISI) channel. In this paper, a soft–output trellis–based equalizer is proposed, taking into account the cyclic ISI structure arising in SC–FDMA, which is especially suited for turbo–encoded transmission over channels with low–to–moderate signal–to–noise ratios (SNRs). A preprocessing stage is necessary for the trellis–based equalizer consisting of a minimum mean–squared error (MMSE) MIMO linear equalizer and a MIMO prediction–error filter, whose design is addressed. Simulation results for an LTE scenario demonstrate that the novel receiver yields significant gains compared to MMSE linear equalization in particular for square MIMO systems.**

I. Introduction

For the uplink of the E–UTRA Long Term Evolution (LTE) mobile communications system, single–carrier frequency–division multiple access (SC–FDMA) transmission, also referred to as discrete Fourier transform (DFT) spread orthogonal frequency division multiplexing (OFDM), has been selected in standardization [1]. A major advantage of SC–FDMA compared to standard OFDM, which is employed in the downlink of LTE, is its reduced peak–to–average power ratio (PAPR) enabling a low–complexity implementation of the mobile terminal and improved performance especially at the cell edge [2], [3]. SC–FDMA will be used in conjunction with multiple–input multiple–output (MIMO) transmission, which plays an important role in LTE in order to improve coverage and capacity [4]. In the receiver at the base station, frequency–domain minimum mean–squared error (MMSE) linear equalization [3], [5] or block–iterative decision–feedback equalization (BI–DFE) [6]–[8] might be applied. In [8], it has been shown that the uncoded bit error rate (BER) of BI–DFE can approach the matched filter bound for increasing signal–to–noise ratio (SNR).

In this paper, we introduce an alternative, noniterative receiver for SC–FDMA transmission over a frequency–selective MIMO channel producing intersymbol interference (ISI). Our approach is motivated by the fact that for a turbo–encoded transmission as applied in LTE, also low–to–moderate SNRs are relevant. In addition, the equalizer should deliver soft output of high quality for subsequent channel decoding. In order to achieve this, our receiver is an approximation to optimum soft–output trellis–based multiuser equalization for SC–FDMA. For this, the standard BCJR algorithm [9] has to be modified due to the equivalent cyclic ISI channel arising in SC–FDMA transmission, which can be done by invoking results from [10] on decoding of tailbiting convolutional codes. Furthermore, because the equivalent channel has a high number of pre- and postcursor taps resulting from a rectangular window in frequency domain in SC–FDMA, a suitable prefiltering technique has to be applied together with state reduction approaches in order to limit the complexity of trellis–based equalization. For prefiltering, we propose the cascade of an MMSE MIMO linear equalizer and a suitably designed MIMO prediction–error filter. Simulation results demonstrate that the novel receiver performs significantly better than a linear equalizer for a turbo–encoded LTE transmission with moderate–to–high code rates at the expense of an increased complexity, which, however, might be tolerable at the base station.

The paper is organized as follows. In Section II, the adopted system model for an SC–FDMA transmission over a frequency–selective MIMO channel is introduced. In Section III, MMSE linear equalization of MIMO channels is revisited for SC–FDMA and some properties of error variances and bias coefficients are highlighted. In Section IV, it is shown that MMSE linear equalization in conjunction with prediction–error filtering is a suitable preprocessing technique for reduced–state trellis–based equalization. Furthermore, it is demonstrated how the BCJR algorithm can be modified in order to be able to cope with cyclic ISI. Sections V and VI provide numerical results and conclusions, respectively.

Notation: $\mathcal{E}\{\cdot\}$, $(\cdot)^T$ and $(\cdot)^H$ stand for expectation, transposition and Hermitian transposition, respectively. Bold lower case letters and bold upper case letters refer to column vectors and matrices, respectively. An exception are frequency–domain vectors for which also bold upper case letters are used. $||\cdot||$ is the L_2–norm of a vector, and $[\boldsymbol{A}]_{m,n}$ stands for the element in the mth row and nth column of $\boldsymbol{A}$. $\boldsymbol{0}_{X\times Y}$ and $\boldsymbol{I}_X$ are the all–zero matrix of size $X \times Y$ and the $X \times X$ identity matrix; $\boldsymbol{\iota}_m$ is a unit column vector with a one at the mth position. $\mathrm{diag}\{x_1, x_2, \ldots, x_n\}$ and $\mathrm{bdiag}\{\boldsymbol{X}_1, \boldsymbol{X}_2, \ldots, \boldsymbol{X}_n\}$ denote a diagonal and a (square or nonsquare) block diagonal matrix with elements $x_1, x_2, \ldots, x_n$ and $\boldsymbol{X}_1, \boldsymbol{X}_2, \ldots, \boldsymbol{X}_n$ on the main diagonal, respectively. $\Pr\{\cdot\}$ ($\Pr\{\cdot\,|\,\cdot\}$) stands for (conditional) probability.

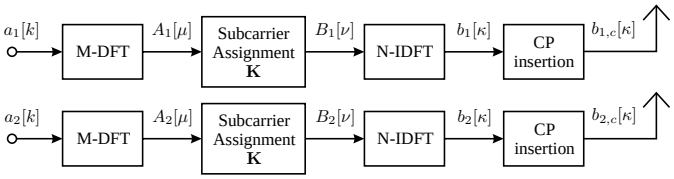

Fig. 1. SC–FDMA transmitter structure.

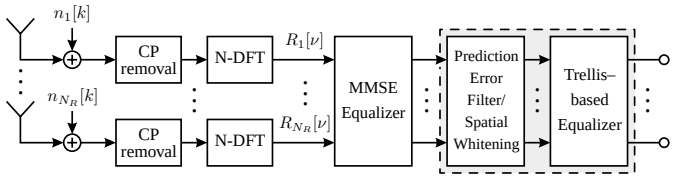

Fig. 2. Considered receiver structure.

II. System Model

We consider a transmission with SC–FDMA modulation over a frequency–selective fading MIMO channel. Transmitter and receiver in discrete–time equivalent complex baseband representation are depicted in Figs. 1 and 2, respectively. Because our focus lies on uplink transmission in LTE where the complexity of the transmitter is limited, $N_T = 2$ transmit antennas and N_R receive antennas are assumed. Nevertheless, the results can be easily generalized to an arbitrary number N_T. The system model in principle is valid for a single–user MIMO transmission with $N_T = 2$ transmitted data streams as well as a (synchronous) multi–user transmission of $N_T = 2$ users equipped with a single antenna each. Both scenarios are relevant for LTE [3]. Simulation results will be given only for the single–user case, where the two transmitted data streams are jointly encoded. After channel coding, interleaving and Gray mapping to the points of a quadrature amplitude modulation (QAM) signal constellation, where 4QAM and 16QAM are the most relevant choices for LTE, $N_T = 2$ sequences of length M are obtained, where the ith sequence, $i \in \{1, 2\}$, has independent, identically distributed (i.i.d.) coefficients $a_i[k]$, $k \in \{0, 1, \ldots, M-1\}$ of variance $\sigma_a^2 = \mathcal{E}\left\{|a_i[k]|^2\right\}$. An M–point DFT is applied to each sequence $a_i[k]$, resulting in $\boldsymbol{A}_i \triangleq \boldsymbol{W}\,\boldsymbol{a}_i$, with $\boldsymbol{A}_i = [A_i[0]\, A_i[1] \ldots A_i[M-1]]^T$, $\boldsymbol{a}_i \triangleq [a_i[0]\, a_i[1] \ldots a_i[M-1]]^T$, and the unitary M–point DFT matrix $\boldsymbol{W}$, $[\boldsymbol{W}]_{\mu,k} = 1/\sqrt{M}\,\mathrm{e}^{-j2\pi\mu k/M}$, $\mu, k \in \{0, 1, \ldots, M-1\}$. In LTE, M is an integer multiple of 12, which is the size of a basic block in frequency domain referred to as resource block. Subsequent to the DFT, subcarrier assignment is made according to the LTE standard [1], for which the localized mode and the distributed mode [3] have been proposed. We focus on the former because it is considered as more relevant for LTE currently. In this case, subcarrier assignment generates vectors $\boldsymbol{B}_i \triangleq \boldsymbol{K}\,\boldsymbol{A}_i$, $i \in \{1, 2\}$, with an $N \times M$ assignment matrix

$$\boldsymbol{K} \triangleq \left[\begin{array}{ccc} \boldsymbol{0}^T_{\nu_0 \times M} & \boldsymbol{I}^T_M & \boldsymbol{0}^T_{(N-M-\nu_0)\times M} \end{array}\right]^T, \tag{1}$$

where ν_0 is the starting index of the contiguous discrete frequency band of width M which is assigned to the considered user. Further users are assigned different frequency bands or slots in time domain by scheduling [2] and need not to be taken into account. By an N–point inverse (I)DFT, time–domain transmit vectors $\boldsymbol{b}_i$ with elements $b_i[\kappa]$, $\kappa \in \{0, 1, \ldots, N-1\}$ are calculated, $\boldsymbol{b}_i \triangleq \boldsymbol{V}^H\,\boldsymbol{B}_i$ ($\boldsymbol{V}$: unitary N–point DFT matrix). A cyclic prefix of length L_c is added to vectors $\boldsymbol{b}_i$ and the sequences $b_{i,c}[\kappa]$ corresponding to $\boldsymbol{b}_{i,c} \triangleq [b_i[N-L_c]\, b_i[N-L_c+1] \ldots b_i[N-1]\, \boldsymbol{b}_i^T]^T$ form the OFDM symbol to be transmitted. The signal at the lth receive antenna, $l \in \{1, 2, \ldots, N_R\}$, can be written as

$$r_l[\kappa] = \sum_{i=1}^{2} \sum_{\lambda=0}^{L-1} h_{l,i}[\lambda]\, b_{i,c}[\kappa - \lambda] + n_l[\kappa], \tag{2}$$

where the discrete–time subchannel impulse response $h_{l,i}[\lambda]$ of length L characterizes transmission from the ith transmit antenna to the lth receive antenna including transmit and receiver input filtering. The MIMO channel is assumed to be constant for transmission of each slot consisting of several vectors (OFDM symbols) $\boldsymbol{b}_{i,c}$ but changes randomly from slot to slot. $n_l[\kappa]$ denotes spatially and temporally white Gaussian noise of variance σ_n^2. In the receiver, the cyclic prefix is first removed, eliminating interference between adjacent OFDM symbols if $L_c \geq L-1$, and after an N–point DFT which can be applied without loss of generality as an input stage the received vector $\boldsymbol{R}_l$ at antenna l can be represented as

$$\boldsymbol{R}_l = \sum_{i=1}^{2} \boldsymbol{H}_{l,i}\,\boldsymbol{B}_i + \boldsymbol{N}_l, \tag{3}$$

corresponding to a cyclic convolution, where $\boldsymbol{H}_{l,i} = \mathrm{diag}\{H_{l,i}[0],\, H_{l,i}[1],\, \ldots,\, H_{l,i}[N-1]\}$ with $H_{l,i}[\nu] \triangleq \sum_{\lambda=0}^{L-1} h_{l,i}[\lambda]\,\mathrm{e}^{-j2\pi\nu\lambda/N}$, and $\boldsymbol{N}_l$ is a frequency–domain noise vector.

Further expansion of (3) yields

$$\boldsymbol{R}_l = \sum_{i=1}^{2} \boldsymbol{H}_{l,i}\boldsymbol{K}\,\boldsymbol{W}\,\boldsymbol{a}_i + \boldsymbol{N}_l. \tag{4}$$

Equalization based on vectors $\boldsymbol{R}_l$ delivers log–likelihood ratios (LLRs) for the encoded bits and is followed by deinterleaving and channel decoding.

III. MMSE Linear Equalization

For low–complexity equalization of SC–FDMA signals, MMSE linear filtering can be applied, cf. e.g. [3], [5], which will serve also as a preprocessing stage for the trellis–based equalization scheme presented in Section IV. In this section, we revisit MMSE linear equalization for MIMO SC–FDMA transmission. In particular, we show how the linear equalizer can be realized efficiently and derive some properties of error variances and bias coefficients for SC–FDMA which are needed for computation of LLRs.

For MMSE filtering, we rearrange the elements $R_l[\nu]$ of $\boldsymbol{R}_l$, $l \in \{1, 2, \ldots, N_R\}$, in a vector

$$\tilde{\boldsymbol{R}} \triangleq [R_1[0]\, R_2[0] \ldots R_{N_R}[0]\, R_1[1]\, R_2[1] \ldots R_{N_R}[N-1]]^T, \tag{5}$$

with

$$\tilde{\boldsymbol{R}} = \mathrm{bdiag}\{\boldsymbol{H}[0],\, \boldsymbol{H}[1],\, \ldots,\, \boldsymbol{H}[N-1]\}\,\boldsymbol{E}\cdot \mathrm{bdiag}\{\boldsymbol{K}\,\boldsymbol{W},\, \boldsymbol{K}\,\boldsymbol{W}\}\,[\boldsymbol{a}_1^T\, \boldsymbol{a}_2^T]^T + \tilde{\boldsymbol{N}}, \tag{6}$$

where $[\boldsymbol{H}[\nu]]_{l,i} \triangleq H_{l,i}[\nu]$, $\boldsymbol{E}$ is a $(2\,N) \times (2\,N)$ permutation matrix containing $\boldsymbol{\iota}_{N(i-1)+\nu}^T$ in its $(2\,\nu + (i-1))$th row, $i \in \{1, 2\}$, $\nu \in \{0, 1, \ldots, N-1\}$, and $\tilde{\boldsymbol{N}}$ is a corresponding rearranged frequency–domain noise vector. It is straightforward to show that the MMSE equalizer matrix $\boldsymbol{F}$ producing estimates $\boldsymbol{y}_i$ for vectors $\boldsymbol{a}_i$,

$$[\boldsymbol{y}_1^T\ \boldsymbol{y}_2^T]^T \triangleq \boldsymbol{F}\,\tilde{\boldsymbol{R}}, \tag{7}$$

can be calculated to

$$\begin{aligned}\boldsymbol{F} = {} & \mathrm{bdiag}\{\boldsymbol{W}^H \boldsymbol{K}^H,\, \boldsymbol{W}^H \boldsymbol{K}^H\}\, \boldsymbol{E}^H \cdot \\ & \mathrm{bdiag}\{(\boldsymbol{H}^H[0]\,\boldsymbol{H}[0] + \zeta\,\boldsymbol{I}_2)^{-1},\, (\boldsymbol{H}^H[1]\,\boldsymbol{H}[1] + \zeta\,\boldsymbol{I}_2)^{-1},\, \ldots \\ & \qquad (\boldsymbol{H}^H[N-1]\,\boldsymbol{H}[N-1] + \zeta\,\boldsymbol{I}_2)^{-1}\} \cdot \\ & \quad \mathrm{bdiag}\{\boldsymbol{H}^H[0],\, \boldsymbol{H}^H[1],\, \ldots,\, \boldsymbol{H}^H[N-1]\},\end{aligned} \tag{8}$$

with $\zeta \triangleq \sigma_n^2/\sigma_a^2$, applying e.g. results given in [11] to the problem at hand.

Hence, MMSE equalization can be performed by the cascade of frequency–domain MMSE MIMO filtering applied independently to each frequency component, cf. [12], inverse permutation yielding frequency–domain vectors for both user signals ($\boldsymbol{E}^H$), selection of the relevant frequency components $\nu \in \{\nu_0, \ldots, \nu_0 + M - 1\}$ and reversal of frequency shift by ν_0 ($\boldsymbol{K}^H$), and IDFT operation, resulting in output vectors $\boldsymbol{y}_i = \boldsymbol{a}_i + \boldsymbol{e}_i$, $i \in \{1, 2\}$, where $\boldsymbol{e}_i$ is an error vector.

Using

$$\begin{bmatrix} \Sigma_{11}^2[\nu] & \Sigma_{12}^2[\nu] \\ \Sigma_{21}^2[\nu] & \Sigma_{22}^2[\nu] \end{bmatrix} \triangleq \sigma_n^2\,(\boldsymbol{H}^H[\nu]\,\boldsymbol{H}[\nu] + \zeta\,\boldsymbol{I}_2)^{-1}, \tag{9}$$

the autocorrelation matrix $\boldsymbol{\Phi}_{e_i e_i} \triangleq \mathcal{E}\left\{\boldsymbol{e}_i\,\boldsymbol{e}_i^H\right\}$ of the error vector can be expressed as

$$\boldsymbol{\Phi}_{e_i e_i} = \boldsymbol{W}^H\,\mathrm{diag}\{\Sigma_{ii}^2[\nu_0], \ldots, \Sigma_{ii}^2[\nu_0 + M - 1]\}\,\boldsymbol{W}. \tag{10}$$

$\boldsymbol{\Phi}_{e_i e_i}$ is a circulant matrix with first column given by $1/\sqrt{M}\,\boldsymbol{W}^H\,\mathrm{diag}\{\Sigma_{ii}^2[\nu_0], \ldots, \Sigma_{ii}^2[\nu_0 + M - 1]\}$, cf. [13]. Hence, the error variance in sequence $y_i[k]$ does not depend on k and is

$$\sigma_{e_i}^2 = \frac{1}{M} \sum_{\mu=0}^{M-1} \Sigma_{ii}^2[\nu_0 + \mu]. \tag{11}$$

It is well known that MMSE equalization results in a biased output signal, i.e., $y_i[k] = a_i[k] + e_i[k]$, where $a_i[k]$ and $e_i[k]$ are statistically dependent [14]. Equivalently, we can write $y_i[k] = c_i\,a_i[k] + \bar{e}_i[k]$, where $\bar{e}_i[k]$ is statistically independent of $a_i[k]$ and $c_i = 1 - \sigma_{e_i}^2/\sigma_a^2$. Before calculation of bit LLRs for channel decoding, the bias should be removed from $y_i[k]$, i.e.,

$$y_{i,u}[k] \triangleq \frac{1}{c_i}\,y_i[k] = a_i[k] + e_{i,u}[k] \tag{12}$$

is further processed, with $\sigma_{e_{i,u}}^2 = \sigma_{e_i}^2/c_i$.

Using (11), the bias coefficient can be calculated to

$$\begin{aligned} c_i &= 1 - \frac{1}{\sigma_a^2}\,\frac{1}{M} \sum_{\mu=0}^{M-1} \Sigma_{ii}^2[\nu_0 + \mu] \\ &= \frac{1}{M} \sum_{\mu=0}^{M-1} c_{F,i}[\nu_0 + \mu], \end{aligned} \tag{13}$$

with frequency–domain bias coefficients

$$c_{F,i}[\nu] = 1 - \frac{\Sigma_{ii}^2[\nu]}{\sigma_a^2}. \tag{14}$$

Thus, time–domain error variance and bias coefficient can be expressed as the arithmetic mean of corresponding frequency–domain error variances and bias coefficients, respectively, cf. (11) and (13).[1]

IV. Trellis–based Equalization

MMSE linear equalization is attractive because it can be realized with low complexity by frequency–domain processing. However, its performance may be not sufficiently good for dispersive channels and/or low number of receive antennas. Several enhanced receivers have been already proposed such as block–iterative decision–feedback equalizers [6], [7] which are able to approach the single user matched filter bound for the raw BER (before channel decoding) in the high SNR regime [7] for large MIMO channels. However, for a coded transmission, also low–to–moderate SNRs are relevant, and soft output of high quality is needed for subsequent channel decoding. Therefore, as a noniterative alternative to BI–DFE, we consider reduced–complexity variants of optimum soft–output trellis–based equalizers. For this, a suitable time–domain representation of the received signal has to be introduced. $\boldsymbol{u}_l \triangleq \boldsymbol{W}^H\,\boldsymbol{K}^H\,\boldsymbol{R}_l$, $l \in \{1, 2, \ldots, N_R\}$, is a set of sufficient statistics in time domain for optimum soft–output equalization,

$$\boldsymbol{u}_l = \sum_{i=1}^{2} \boldsymbol{W}^H\,\boldsymbol{K}^H\,\boldsymbol{H}_{l,i}\,\boldsymbol{K}\,\boldsymbol{W}\,\boldsymbol{a}_i + \boldsymbol{w}_l, \tag{15}$$

cf. (4). Here, $\boldsymbol{W}^H\,\boldsymbol{K}^H\,\boldsymbol{H}_{l,i}\,\boldsymbol{K}\,\boldsymbol{W}$ is a circulant matrix related to a circular convolution of $a_i[k]$ with the impulse response

$$g_{l,i}[k] \triangleq \frac{1}{M} \sum_{\mu=0}^{M-1} H_{l,i}[\nu_0 + \mu]\,\mathrm{e}^{j2\pi\mu k/M}, \tag{16}$$

and $\boldsymbol{w}_l$ is a white Gaussian noise vector, $\boldsymbol{w}_l = \boldsymbol{W}^H\,\boldsymbol{K}^H\,\boldsymbol{N}_l$. According to (16), $g_{l,i}[k]$ has a frequency response obtained by rectangular windowing of $H_{l,i}[\nu]$ and subcarrier reassignment (reversal of frequency shift by ν_0). Due to this, additional pre– and postcursor taps arise, and the effective length of $g_{l,i}[k]$ might be significantly larger than the original channel length L. In this case, some preprocessing is required for trellis–based equalization in order to condition the effective overall channel.

A. Prefiltering for Trellis–Based Equalization

For preprocessing, the MMSE MIMO linear equalizer of Section III can be applied in a first stage, eliminating ISI, but introducing spatial and temporal noise correlations. Because MIMO trellis–based equalization adopting the squared Euclidean metric [15] requires a signal impaired by spatially and temporally white Gaussian noise, a finite impulse response (FIR) prediction–error filter of order q_p is employed in a second stage for approximate removal of the temporal noise correlations, reinserting ISI in a controlled manner. q_p should be chosen for a compromise between complexity and performance of trellis–based equalization.

[1] The expression in (9) can be viewed as error autocorrelation matrix of MMSE equalization of $\boldsymbol{H}[\nu]$.

Prediction–error filtering is applied to linear equalizer output vector $\boldsymbol{y}[k] \triangleq [y_1[k]\, y_2[k]]^T$, $\boldsymbol{y}[k] = \boldsymbol{a}[k] + \boldsymbol{e}[k]$, with similar definitions of $\boldsymbol{a}[k]$ and $\boldsymbol{e}[k]$, resulting in an output signal

$$\begin{aligned}\boldsymbol{u}_p[k] &= \boldsymbol{y}[k] - \sum_{\xi=1}^{q_p} \boldsymbol{P}[\xi]\, \boldsymbol{y}[k-\xi],\ k \in \{0,\, 1,\, \ldots,\, M-1\} \\ &= \boldsymbol{a}[k] - \sum_{\xi=1}^{q_p} \boldsymbol{P}[\xi]\, \boldsymbol{a}[k-\xi] + \boldsymbol{w}_p[k], \end{aligned} \tag{17}$$

where the definitions $\boldsymbol{y}[-\xi] \triangleq \boldsymbol{y}[M-\xi]$, $\boldsymbol{a}[-\xi] \triangleq \boldsymbol{a}[M-\xi]$, $\xi \in \{1,\, \ldots,\, q_p\}$ are used in order to establish cyclic convolution. For calculation of the optimum filter coefficient matrices $\boldsymbol{P}[\xi]$ minimizing the variances of components of error signal $\boldsymbol{w}_p[k]$ after filtering, the (cyclic) autocorrelation matrix sequence $\boldsymbol{A}[\xi] \triangleq \mathcal{E}\left\{\boldsymbol{e}[k]\, \boldsymbol{e}^H[k-\xi]\right\}$ of $\boldsymbol{e}[k]$ (with corresponding periodical extension) is required,

$$\boldsymbol{A}[\xi] = \frac{\sigma_n^2}{M} \sum_{\mu=0}^{M-1} \left(\boldsymbol{H}^H[\nu_0+\mu]\, \boldsymbol{H}[\nu_0+\mu] + \zeta\, \boldsymbol{I}_2\right)^{-1} \mathrm{e}^{j2\pi\xi k/M}, \tag{18}$$

cf. (9). Using (18), the optimum prediction–error filter results from

$$\begin{aligned}&\begin{bmatrix} \boldsymbol{A}[0] & \boldsymbol{A}[1] & \ldots & \boldsymbol{A}[q_p-1] \\ \boldsymbol{A}[-1] & \boldsymbol{A}[0] & \ldots & \boldsymbol{A}[q_p-2] \\ \vdots & \vdots & \ddots & \vdots \\ \boldsymbol{A}[-q_p+1] & \boldsymbol{A}[-q_p+2] & \ldots & \boldsymbol{A}[0] \end{bmatrix} \cdot \begin{bmatrix} \boldsymbol{P}^H[1] \\ \boldsymbol{P}^H[2] \\ \vdots \\ \boldsymbol{P}^H[q_p] \end{bmatrix} \\ &\quad = \begin{bmatrix} \boldsymbol{A}^T[-1] & \boldsymbol{A}^T[-2] & \ldots & \boldsymbol{A}^T[-q_p] \end{bmatrix}^T, \end{aligned} \tag{19}$$

which is the multichannel extension of [16, Eqs. (30),(31)]. The error variances and spatial correlations after filtering are given by $\boldsymbol{A}_p \triangleq \mathcal{E}\left\{\boldsymbol{w}_p[k]\, \boldsymbol{w}_p^H[k]\right\} = \boldsymbol{A}[0] - \sum_{\xi=1}^{q_p} \boldsymbol{P}[\xi]\, \boldsymbol{A}[-\xi]$, cf. also [17]. Spatial correlations in $\boldsymbol{w}_p[k]$ can be removed by forming $\bar{\boldsymbol{u}}_p[k] \triangleq \boldsymbol{G}^{-1}\, \boldsymbol{u}_p[k]$, where $\boldsymbol{G}$ results from Cholesky factorization of $\boldsymbol{A}_p$, $\sigma_n^2\, \boldsymbol{G}\, \boldsymbol{G}^H = \boldsymbol{A}_p$. $\bar{\boldsymbol{u}}_p[k]$ serves as input of trellis–based equalization.

B. Soft–Output Trellis–Based Equalization Algorithm

A BCJR algorithm [9] delivering soft output in contrast to the standard Viterbi algorithm can be applied to signal $\bar{\boldsymbol{u}}_p[k]$, running in a trellis diagram with states defined as

$$\tilde{\boldsymbol{S}}[k] \triangleq [\tilde{\boldsymbol{a}}^T[k-1]\ \ldots\ \tilde{\boldsymbol{a}}^T[k-q_p]]^T, k \in \{0, 1, \ldots, M-1\}, \tag{20}$$

where $\tilde{\boldsymbol{a}}[k-\xi]$ denote hypothesis vectors of trellis-based equalization. The BCJR algorithm calculates a posteriori probabilities $\Pr\{a_i[k] \,|\, \{\bar{\boldsymbol{u}}_p[\xi],\, \xi \in \{0,\, 1,\, \ldots,\, M-1\}\}$ employing the quantities $\alpha_k(\tilde{\boldsymbol{S}}[k]) \triangleq \Pr\{\tilde{\boldsymbol{S}}[k], \{\bar{\boldsymbol{u}}_p[\xi],\, \xi \in \{0,\, 1,\, \ldots,\, k\}\}$ and $\beta_k(\tilde{\boldsymbol{S}}[k]) \triangleq \Pr\{\tilde{\boldsymbol{S}}[k] \,|\, \{\bar{\boldsymbol{u}}_p[\xi],\, \xi \in \{k+1,\, k+2,\, \ldots,\, M-1\}\}$ defined as usual for the BCJR algorithm [9]. Both quantities can be computed with a forward and backward recursion, respectively, in which a branch factor $\lambda_k(\tilde{\boldsymbol{S}}[k-1],\, \tilde{\boldsymbol{S}}[k]) \triangleq \Pr\{\tilde{\boldsymbol{S}}[k],\, \bar{\boldsymbol{u}}_p[k] \,|\, \tilde{\boldsymbol{S}}[k-1]\}$ is needed, where

$$\begin{aligned}\lambda_k(\tilde{\boldsymbol{S}}[k-1],\, \tilde{\boldsymbol{S}}[k]) \sim \exp\Big(-\Big\|\bar{\boldsymbol{u}}_p[k] - \boldsymbol{G}^{-1}\, \tilde{\boldsymbol{a}}[k] \\ + \sum_{\xi=1}^{q_p} \boldsymbol{G}^{-1}\, \boldsymbol{P}[\xi]\, \tilde{\boldsymbol{a}}[k-\xi]\Big\|^2 \Big/ \sigma_n^2\Big) \end{aligned} \tag{21}$$

for all allowed transitions in the trellis diagram. A major difference to standard soft–output equalization arises due to the cyclic ISI in $\bar{\boldsymbol{u}}_p[k]$. Therefore, $\boldsymbol{S}[0] \equiv \boldsymbol{S}[M]$ holds, imposing a cyclic structure on the trellis diagram which has neither origin from nor termination in a definite state given e.g. by tail symbols. A similar problem is known in soft–output decoding of tailbiting convolutional codes [10]. The main task to be solved is to find suitable initializations for the forward and backward recursion, respectively, i.e., values $\alpha_0(\tilde{\boldsymbol{S}}[0])$ and $\beta_M(\tilde{\boldsymbol{S}}[M])$. In [10], it is shown that vector $\boldsymbol{\alpha}_0$ containing all initial α's is given by the eigenvector pertaining to the largest eigenvalue of matrix $\boldsymbol{\Gamma} \triangleq \boldsymbol{\Gamma}_{M-1} \ldots \boldsymbol{\Gamma}_0$, where matrices $\boldsymbol{\Gamma}_k$ contain the branch factors $\lambda_k(\tilde{\boldsymbol{S}}[k-1],\, \tilde{\boldsymbol{S}}[k])$ for all state transitions at time k. In order to initialize the backward recursion, a similar eigenvalue problem can be set up for vector $\boldsymbol{\beta}_N$. These results of [10] for tailbiting convolutional codes can be directly transferred to the problem at hand, using the branch factors of (21) in $\boldsymbol{\Gamma}_k$. In order to circumvent the computational complexity associated with direct eigenvalue decomposition of $\boldsymbol{\Gamma}$, an alternative solution has been proposed in [10], which is based on the fact that repeated multiplication of an arbitrary (nonzero) vector with matrix $\boldsymbol{\Gamma}$ gives a vector that converges to the eigenvector pertaining to the largest eigenvalue of $\boldsymbol{\Gamma}$. On the other hand, because $\boldsymbol{\alpha}_M = \boldsymbol{\Gamma}\, \boldsymbol{\alpha}_0$, this recursion is equivalent to several forward recursions through the trellis diagram, where the (normalized) final $\boldsymbol{\alpha}$ vector of the current run serves as initial vector for the next run. After convergence, the result is taken for initialization of a final forward recursion. A similar statement is valid for $\boldsymbol{\beta}_N$, which is initialized by some preliminary backward recursions. Both recursions converge quite fast, which can be exploited for the design of a practical algorithm with limited additional complexity [10]. For this, the prefiltered signal block is augmented e.g. with its second half to the left and its first half to the right. To the resulting block, a BCJR algorithm is applied with arbitrary, e.g. uniform initialization of α's and β's, and a posteriori probabilities of symbols and bit LLRs are calculated from the α's and β's of the middle part of the augmented block.

Even for moderate prediction orders, complexity of the BCJR algorithm may become prohibitively high because the number of trellis states is given by $Z = 16^{q_p}$ and $Z = 256^{q_p}$ for 4QAM and 16QAM, respectively. Hence, a small q_p should be selected ($q_p = 1 - 2$) or a reduced–complexity BCJR algorithm based on the principles of delayed decision–feedback or reduced–state sequence estimation might be applied, which can be specified in a straightforward manner via the principles given e.g. in [18], [19], resulting in a modified computation of branch factors involving decision feedback. It should be noted that the proposed prefiltering approach results in a minimum–phase overall MIMO channel [20] which is well suited for state reduction.

C. Computational Complexity

The complexity of the proposed trellis–based equalizer is mainly determined by that of calculation of the optimum prediction–error filter and subsequent filtering, and complexity

of the used BCJR algorithm. For prediction–error filter calculation, the block Levinson algorithm can be applied which requires $\mathcal{O}(q_p^2)$ operations. Complexity of the BCJR algorithm is basically twice that of a Viterbi algorithm because a forward and a backward recursion is required, and is proportional to the number of considered trellis branches per time step which is 16^{q_p+1} for $N_T = 2$, 4QAM and a full–state algorithm. Also, it should be noted that because augmented blocks have to be processed in order to take into account cyclic ISI, complexity is increased correspondingly compared to a standard BCJR algorithm. The complexity of MMSE equalization, which is used as a first stage in the proposed scheme, is mainly governed by the inversion of 2×2 matrices in (8) and DFT/IDFT operations. In summary, complexity of the novel scheme is considerably higher than that of MMSE equalization. Nevertheless, a higher receiver complexity might be tolerable in the uplink (i.e., at the base station) if a noticeable performance gain results.

V. Simulation Results

For simulations, the generic frame structure of the frequency division duplex (FDD) mode of LTE [1] is considered. Here, channel coding using a Turbo code according to the UMTS standard [4] with code rate R_c is done over a frame comprising two slots, where each slot contains 7 OFDM symbols. Both slots are transmitted in parallel over the two antennas. The DFT sizes are selected to $M = 300$ and $N = 512$, and $\nu_0 = 0$. The length of the cyclic prefix is $L_c = 144$. Different subchannels of the MIMO channel are assumed as independent. A MIMO flat fading channel and two MIMO ISI channels are considered, where each subchannel of the ISI channels has a power delay profile which is a discrete approximation of that of the 3GPP Pedestrian A and Pedestrian B channel, respectively. In all cases, $q_p = 1$ has been chosen for prediction–error filtering, and a full–state BCJR algorithm taking into account the cyclic ISI has been used. Perfect channel knowledge has been assumed. Simulations have been also performed for $q_p > 1$ and a reduced–complexity BCJR algorithm (results not shown). A worse performance is observed in this case for coded transmission. This is because for the considered scenarios, a significant part of the maximum possible prediction gain can be already obtained for $q_p = 1$ and soft output of the reduced–complexity algorithm is degraded due to error propagation.

In Fig. 3, the frame error rate (FER) after channel decoding versus E_b/N_0 (E_b: average received bit energy per antenna, N_0: single–sided power spectral density of the underlying continuous–time passband noise) is shown for the conventional MMSE linear equalizer and the proposed equalizer, respectively, where the flat fading channel, QPSK, $R_c = 1/2$, and $N_R \in \{2, 4\}$ were used. The novel equalizer achieves a gain of 5 dB compared to the conventional equalizer at $\mathrm{FER} = 10^{-2}$ for $N_R = 2$. In the flat fading case, the novel receiver in principle is optimum, in contrast to the linear equalizer which introduces noise enhancement by spatial filtering. For $N_R = 4$, the gain of the novel receiver is reduced to 0.8 dB as in the case of more receive than transmit antennas, linear equalization can avoid excessive noise enhancement.

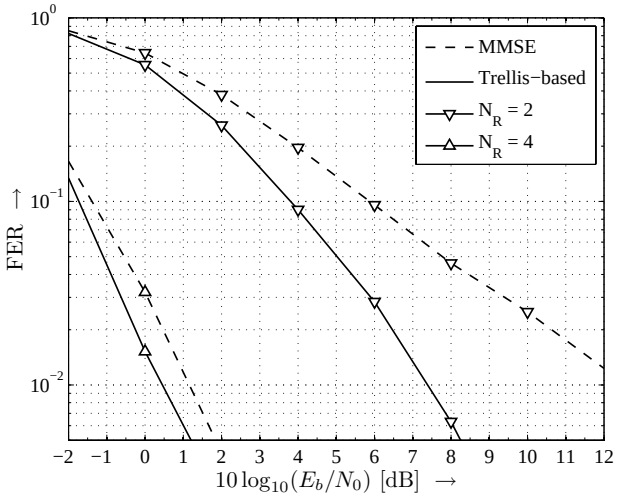

Fig. 3. FER of novel trellis–based receiver and conventional linear equalizer, respectively, versus $10\log_{10}(E_b/N_0)$. QPSK, flat fading channel, $R_c = 1/2$, $N_R \in \{2, 4\}$.

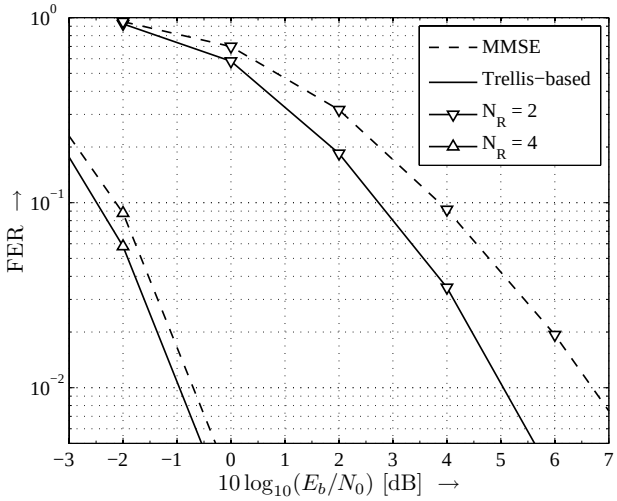

Fig. 4. FER of novel trellis–based receiver and conventional linear equalizer, respectively, versus $10\log_{10}(E_b/N_0)$. QPSK, Pedestrian A channel, $R_c = 1/2$, $N_R \in \{2, 4\}$.

Fig. 4 is valid for the Pedestrian A channel. Otherwise, the same scenario as for Fig. 3 has been selected. For $N_R = 2$, the novel receiver gains 1.8 dB at $\mathrm{FER} = 10^{-2}$ compared to the conventional equalizer. For $N_R = 4$, the gain is again reduced. In general, the gains of the novel receiver are still significant for ISI channels but not as high as for the flat fading channel, because the linear equalizer can utilize temporal diversity of the ISI channel. This is confirmed by Fig. 5, which is valid for 16QAM, the Pedestrian A channel, $R_c = 1/2$ and $N_R = 2$.

Finally, the results shown in Fig. 6 for the more dispersive Pedestrian B channel, QPSK transmission, $N_R = 2$, and $R_c \in \{1/3, 1/2\}$ indicate that the novel receiver is mainly beneficial if protection due to channel coding is not too strong, i.e., if moderate–to–high code rates are used corresponding to high bandwidth efficiency. For low code rates, the SNR at the equalizer input is very low for FERs after channel decoding of

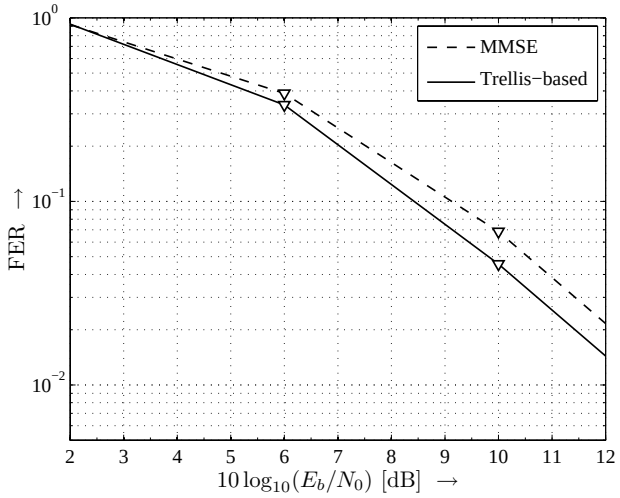

Fig. 5. FER of novel trellis–based receiver and conventional linear equalizer, respectively, versus $10\log_{10}(E_b/N_0)$. 16QAM, Pedestrian A channel, $R_c = 1/2$, $N_R = 2$.

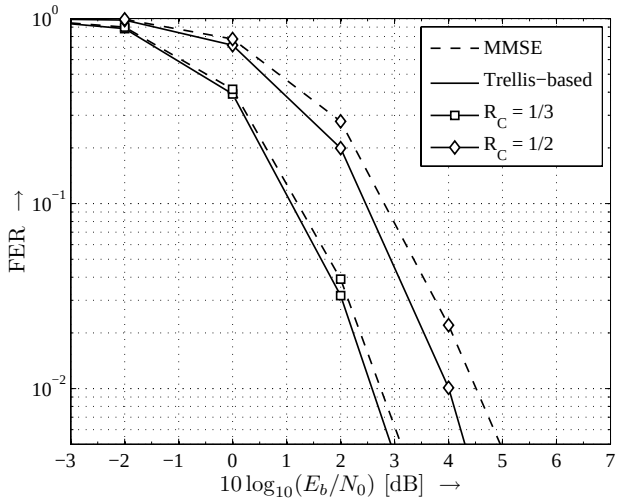

Fig. 6. FER of novel trellis–based receiver and conventional linear equalizer, respectively, versus $10\log_{10}(E_b/N_0)$. QPSK, Pedestrian B channel, $N_R = 2$, $R_c \in \{1/2,\ 1/3\}$.

practical interest. It is well known that in this regime, MMSE equalization in general has a performance close to that of the optimum receiver.

VI. Conclusions

In this paper, we have proposed a novel soft–output trellis–based equalization algorithm for an SC–FDMA transmission over MIMO ISI channels which is an approximation to the theoretically optimum receiver. In algorithm design, the cyclic ISI and the unfavorable equivalent channel, which are both due to SC–FDMA modulation, have been taken into account by a tailbiting BCJR algorithm and a preprocessing stage with cyclic filtering, respectively. For the latter, it has been shown that the cascade of an MMSE equalizer and a prediction–error filter is a good choice. The design of both filters for SC–FDMA has been addressed, and interesting properties of the MMSE filter have been unveiled. The novel receiver delivers soft output of better quality than that of the MMSE MIMO linear equalizer in particular for square (e.g. 2×2) MIMO systems as demonstrated by simulation results for a typical LTE transmission with turbo coding.

References

[1] *3GPP TS 36.211, Evolved Universal Terrestrial Radio Access (E-UTRA), Physical Channels and Modulation (Release 8)*, 3GPP, Jun. 2007.

[2] H. Myung, J. Lim, and D. Goodman, "Single Carrier FDMA for Uplink Wireless Transmission," *IEEE Vehicular Technology Magazine*, vol. 1, pp. 30–38, Sep. 2006.

[3] T. Lunttila, J. Lindholm, K. Pajukoski, E. Tiirola, and A. Toskala, "EUTRAN Uplink Performance," in *Proceedings of the International Symposium on Wireless Pervasive Computing (ISWPC'07)*, San Juan, Puerto Rico, Jan. 2007, pp. 515–519.

[4] H. Ekström, A. Furuskär, J. Karlsson, M. Meyer, S. Parkvall, J. Torsner, and M. Wahlqvist, "Technical Solutions for the 3G Long–Term Evolution," *IEEE Communications Magazine*, vol. 44, pp. 38–45, Mar. 2006.

[5] B. Priyanto, H. Codina, S. Rene, T. Sørensen, and P. Mogensen, "Initial Performance Evaluation of DFT–Spread OFDM Based SC–FDMA for UTRA LTE Uplink," in *Proceedings of IEEE Vehicular Technology Conference (VTC-Spring 2007)*, Dublin, Ireland, Apr. 2007, pp. 3175–3179.

[6] R. Dinis, D. Falconer, C. Lam, and M. Sabbaghian, "A Multiple Access Scheme for the Uplink of Broadband Wireless Systems," in *Proceedings of the IEEE Global Telecommunications Conference (Globecom'04)*, Dallas, TX, Nov./Dec. 2004, pp. 3808–3812.

[7] Y. Pei and Y.-C. Liang, "Subcarrier–Based Block–Iterative GDFE (BI–GDFE) Receivers for MIMO Interleaved FDMA," in *Proceedings of IEEE Vehicular Technology Conference (VTC-Spring 2007)*, Dublin, Ireland, Apr. 2007, pp. 2033–2037.

[8] R. Kalbasi, R. Dinis, D. Falconer, and A. Banihashemi, "An Iterative Frequency–Domain Layered Space–Time Receiver for SDMA Systems with Single–Carrier Transmission," in *Proceedings of IEEE International Conference on Acoustics, Speech, and Signal Processing (ICASSP'04)*, Montreal, Canada, May 2004, pp. IV–793–IV–796.

[9] L. Bahl, J. Cocke, F. Jelinek, and J. Raviv, "Optimal Decoding of Linear Codes for Minimizing Symbol Error Rate," *IEEE Transactions on Information Theory*, vol. 20, pp. 284–287, Mar. 1974.

[10] J. Andersen and S. Hladik, "Tailbiting MAP Decoders," *IEEE Journal on Selected Areas in Communications*, vol. 16, pp. 297–302, Feb. 1998.

[11] A. Hedayat, A. Nosratinia, and N. Al-Dhahir, "Linear Equalizers for Flat Fading Rayleigh MIMO Channels," in *Proceedings of IEEE International Conference on Acoustics, Speech, and Signal Processing (ICASSP'05)*, Philadelphia, PA, Mar. 2005, pp. III/445 – III/448.

[12] D. Falconer, S. Ariyavisitakul, A. Benyamin-Seeyar, and B. Eidson, "Frequency–Domain Equalization for Single–Carrier Broadband Systems," *IEEE Communications Magazine*, vol. 40, pp. 58–66, Apr. 2002.

[13] G. Golub and C. Van Loan, *Matrix Computations*. The John Hopkins University Press, 1990.

[14] J. Cioffi, G. Dudevoir, M. Eyuboglu, and G. D. Forney, Jr., "MMSE Decision-Feedback Equalizers and Coding – Parts I and II," *IEEE Trans. on Commun.*, vol. 43, pp. 2582–2604, Oct. 1995.

[15] W. V. Etten, "Maximum Likelihood Receiver for Multiple Channel Transmission Systems," *IEEE Trans. on Commun.*, pp. 276–283, Feb. 1976.

[16] N. Benvenuto and S. Tomasin, "On the Comparison Between OFDM and Single Carrier Modulation With a DFE Using a Frequency–Domain Feedforward Filter," *IEEE Trans. on Commun.*, vol. 50, pp. 947–955, Jun. 2002.

[17] B. Friedlander, "Lattice Filters for Adaptive Processing," *Proceedings of the IEEE*, vol. 70, pp. 829–867, Aug. 1982.

[18] P. Höher, "TCM on Frequency-Selective Fading Channels: A Comparison of Soft-Output Probabilistic Equalizers," in *Proceedings of the IEEE Global Telecommunication Conference (GLOBECOM'90)*, San Diego, Dec. 1990, pp. 401.4.1.–401.4.6.

[19] G. Colavolpe, G. Ferrari, and R. Raheli, "Reduced–State BCJR–Type Algorithms," *IEEE Journal on Selected Areas in Communications*, vol. 19, pp. 848–859, May 2001.

[20] D. Youla and N. Kazanjian, "Bauer-Type Factorization of Positive Matrices and the Theory of Matrix Polynomials Orthogonal on the Unit Circle," *IEEE Transactions on Circuits and Systems*, vol. 25, pp. 57–69, Feb. 1978.